Shock Boundary Layer Interaction in Internal Flow: Dependence on the Method of Throttling

Balaji A Himakar[1] and Srisha M V Rao[1,*]
1: Dept. of Aerospace Engineering, Indian Institute of Science, Bangalore, India
* Corresponding author: srisharao@iisc.ac.in

Keywords: Shock boundary layer interaction, shock train, supersonic co-flow, mechanical throttling

ABSTRACT

Supersonic co-flow configuration occurs in multiple cases such as dual combustor ramjet (DCR) engine, rocket-based combined cycle (RBCC) engine, high altitude test facilities (HATF) and supersonic-supersonic ejectors (SSE). The high momentum jet of the core flow in an under-expanded state creates fluidic blockage enough to throttle the peripheral supersonic flow leading to shock train formation as shown in the schematic in figure 1(a). Shock train is an outcome of shock boundary layer interaction in the confined duct (isolator) under an adverse pressure gradient. The isolator duct length sizing becomes a formidable design challenge in the overall design of the system as it has to retain the shock train within itself, avoiding underperformance of any of the upstream components.

Ground test facilities used to study shock trains in general employ mechanical throttling with a flap or a butterfly valve[1-3] to throttle the flow downstream of the isolator. Fluidic throttling on the other hand in addition to the area blockage and pressure imposition, shall have additional complexities such as mixing layer, entrainment, vortex shedding, etc., that may further affect the shock train's statics and dynamics. The work on shock train in co-flow configuration [4-5] was performed on the axisymmetric test setups, where the outcome relied on the sparsely distributed static pressure data and no visual confirmation of the flow features exists. Though the empirical correlation developed for shock train length in the case with mechanical flaps [1] was compared with the experimentally obtained shock train length in annular duct with fluidic throttling [4-5] and was observed that they don't match well, a thorough quantification of differences and possible reasons for deviation was not reported.

Hence, a comparative study of fluidic throttling against mechanical throttling over a similar setup is required for a better understanding of the differences in the SBLI and its dependence on the method of throttling. This research gap forms the basic motivation of this work to understand the mechanism and causality of the shock train dynamics in a co-flow setup as compared to the mechanical throttling case. This requires designing an optically diagnosable setup that can provide the visualization of the flow features along with point measurements of the wall static pressure data, thus leading to a choice of the rectangular cross-section setup.

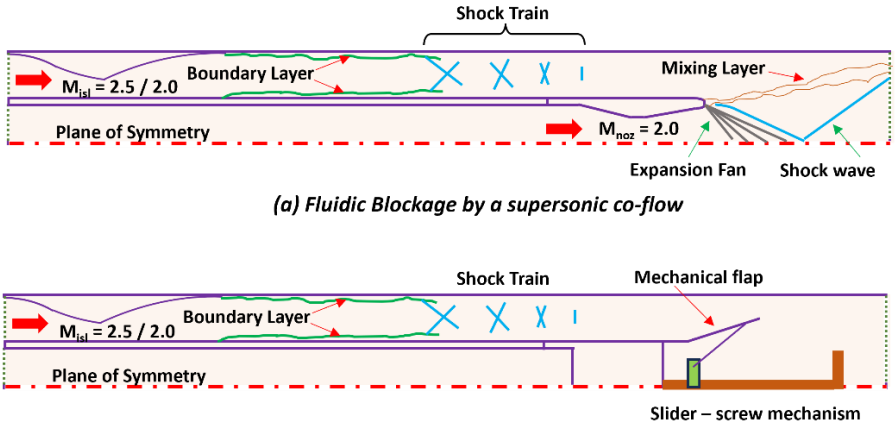

Figure 1 Schematic of the mechanism and possible flow features in (a) the supersonic co-flow and (b) the mechanical flap.

A modular test section that can be used for both co-flow configuration, as well as mechanical throttling, is designed to be adaptable to the existing pressure-vacuum-based direct connect facility. The isolator duct has a rectangular section of an aspect

ratio 5 and non dimensional duct length of 20 (non-dimensionalized with duct height). The supersonic flow in the isolator is generated by a contoured nozzle of design Mach number 2.0 stationed upstream of the duct to provide a uniform flow entering the isolator. The duct that carries core flow (denoted a nozzle) can be attached with a convergent-divergent nozzle to generate a supersonic flow, in the present case it is of design Mach number 2.0 as shown in figure 1(a). Stagnation pressures of both core flow and isolator flow are regulated independently and the choice of the stagnation pressures is made such that the shock train is stationed within the isolator duct at various axial locations and the core flow is under expanded. Similarly, the mechanical flap module actuated using the slider-screw mechanism can be attached to the duct carrying the core flow at the same location where the nozzle was attached as shown in figure 1(b). The slider-screw mechanism that actuates the flap provides a range of solid blockage ratios. Though the initial attempt was to set the flap geometry to mimic the perceived mixing layer edge in the case of fluidic throttling, the duct never started at those blockage ratios. Thus, the area blockage ratio is reduced till a started case is achieved and the shock train can be stationed in the duct. For the present case, 26% area blockage is chosen and isolator stagnation pressure is varied to position the shock train inside the isolator at various axial locations.

High-speed schlieren imaging and wall static pressure measurements constitute the diagnostics. The Z-type configuration-based high-speed schlieren imaging is employed with Si-LUX 640 nano pulsed laser as the light source and Photron SA4 camera for image recording. Each frame is exposed with a 10 ns width of laser pulse illumination and recorded at the rate of 20,000 frames per second. The exposure of the camera sensor and the pulsing of the laser were synchronized using a digital delay pulse generator. The wall static pressure taps provided on the top wall of the test section were connected to MPX make semiconductor based piezo resistive type pressure transducers using silicone rubber tubing. Pressure signal from each sensor is acquired using an eight-channel Picoscope at a rate of 50,000 samples per second.

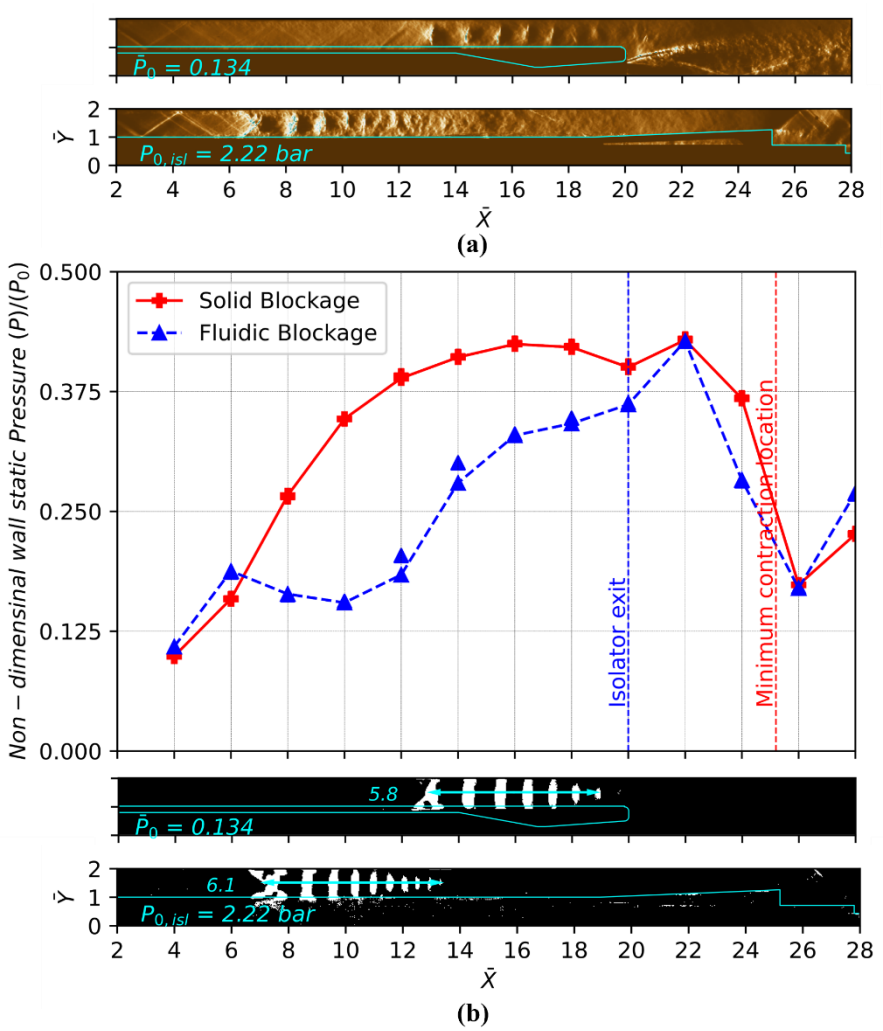

Figure 2 (a) Instantaneous schlieren image (b) time-averaged wall static pressure and zero lag correlation map of STLE signal with time series signal of each pixel of schlieren images. Images are shown for both co-flow and mechanical flap cases.

Among various cases in fluidic blockage and solid blockage cases, one case in each is picked, that has the same overall adverse pressure ratio of approximately 2.6. Instantaneous schlieren images of isolator flow with both fluidic blockage and solid

blockage are shown in figure 2(a). The setup geometry's surface edges are overdrawn on the schlieren images in cyan color for better understanding. The schlieren image itself has been captured in monochrome and is represented in the 'BrBG' color map for enhanced visual representation. The shock train leading edge's (STLE) time trace signal is extracted for a 250 ms time interval from schlieren images and it is cross-correlated with each pixel's time signal in the schlieren images of the same time interval. Thus obtained zero-lag cross-correlation map is strongly correlated only with the shock train and weekly correlated with other features like the mixing layer, mixing region in the pseudo shock, shocks from the core flow, etc.. Thus, carefully thresholding leads to the shock train alone which is represented in figure 2(b). Time-averaged non-dimensional wall static pressure distribution is also represented in figure 2(b) where the geometrical reference lengths are also represented.

Initial observations indicate that for the same adverse pressure ratio of 2.6, the shock train leading edge(STLE) is stationed upstream for the case of solid blockage when compared to the fluidic blockage by around 6 times duct height distance. The same can be observed in the pressure distribution as well. The shock train length within the overall pseudo shock appears to be of similar lengths, but the overall number of shocks in the shock train is more and thus closely packed in a solid blockage case as compared to the fluidic blockage.

The major attribution for these deviations can be directed to the entrainment effect caused by the high momentum core flow in the fluidic blockage case. Further, data-driven analysis such as POD, SPOD, and spectral analysis on the pressure data and the STLE shall be performed to get a better understanding of the causality of the differences, which shall be presented in this work.

REFERENCES

1. Waltrup, P. J., & Billig, F.S. (1973). Structure of shock waves in cylindrical ducts. AIAA J. 11(10), 1404-1408.
2. Hunt, R., and Gamba, M. (2019). On the origin and propagation of perturbations that cause shock train inherent unsteadiness. J. Fluid fMech. 861, 815-859.
3. Nan, L., Chang, J., Xu, K., Yu D., Bao, W., & Song, Y. (2018). Oscillation of the shock train in an isolator with incident shocks. Physics of Fluids 30(11).
4. Stockbridge, R. D. (1988). Experimental investigation of shock wave boundary layer interactions in an annular duct. J. Propulsion 5(3).
5. Byun, J., Park, C., Kwon, O. J., & Ahn, J. (2015). Experimental study of combustor isolator interactions in a dual combustion ramjet. J. Propulsion and Power 31(2).